Nano Energy (2015) 14, 111–125

Available online at www.sciencedirect.com

ScienceDirect

journal homepage: www.elsevier.com/locate/nanoenergy

RAPID COMMUNICATION

Self-powered flexible inorganic electronic system

Seung Hyun Lee[1], Chang Kyu Jeong[1], Geon-Tae Hwang, Keon Jae Lee*

Department of Materials Science and Engineering, Korea Advanced Institute of Science and Technology (KAIST), 291 Daehak-ro, Yuseong-gu, Daejeon 305-701, Republic of Korea

Received 14 October 2014; accepted 6 December 2014
Available online 13 December 2014

KEYWORDS
Flexible inorganic electronics;
Flexible optoelectronics;
Flexible large scale integration;
Self-powered system;
Flexible energy sources;
Laser material interaction

Abstract
Self-powered flexible inorganic electronic systems have been demonstrated to be the core of next-generation electronics due to their lightweight, thin, self-sustainable and biocompatible properties, which are applicable to cramped or corrugated surfaces. Many researchers have studied myriad approaches for high performance flexible electronics, *e.g.* energy harvesters, batteries, high-density memories, large-scale integration (LSI), light-emitting diodes (LEDs), and sensors. Moreover, innovative devices for *in vivo* biomedical applications have been demonstrated on curvilinear and isolated regions of human bodies for detecting or even treating diseases. This paper reviews recent advances in self-powered flexible inorganic electronics, covering material selection, mechanical design, fabrication method and their all-in-one integration on a single plastic substrate.

Introduction

The inorganic based semiconductor industry has led epoch-making advances in information technology (IT) for the past half century. During that time, the main focus of modern electronics has been pursuit of high performance, large size and huge energy-consuming applications such as data servers and personal computers. Recently, with the advent of high-tech flexible technologies, future electronics will change this paradigm to lightweight, thin, flexible and self-powered systems with human-friendly interfaces.

Many researchers have demonstrated advanced approaches to self-powered flexible inorganic devices, including energy harvesters [1,2], batteries [3,4], high-density memories [5,6], large-scale integration (LSI) [7,8], light-emitting diodes (LEDs) [9,10], and sensors [11–13]. In addition, there have been several efforts to realize multifunctional self-powered flexible systems that combine these flexible units on a single plastic substrate [14,15]. Such systems can be placed on unconventional surfaces

*Corresponding author. Tel.: +82 42 350 3343.
E-mail address: keonlee@kaist.ac.kr (K.J. Lee).
[1]These authors contributed equally to this work.

http://dx.doi.org/10.1016/j.nanoen.2014.12.003
2211-2855/

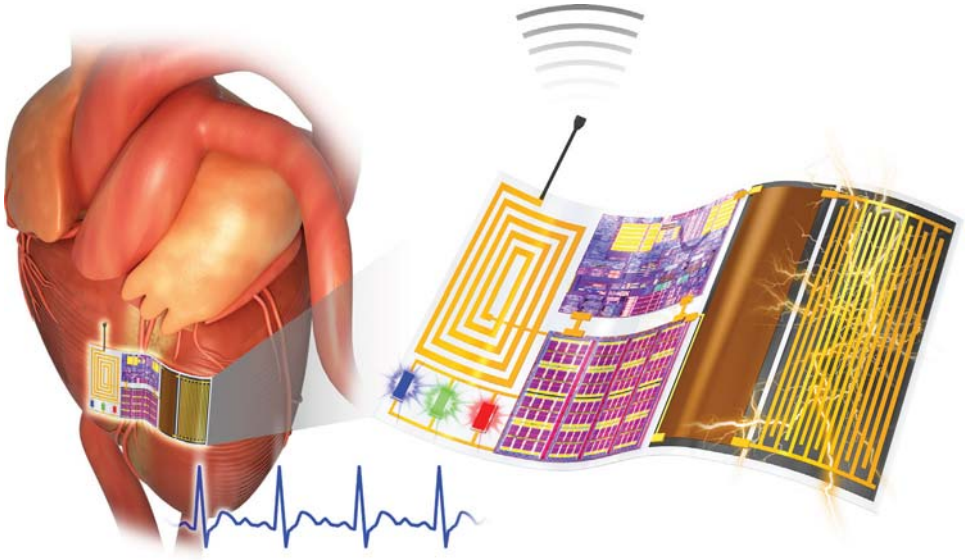

Figure 1 Schematic illustration of self-powered flexible inorganic electronic systems.

where traditional bulk devices are difficult to access and install, such as spatially-isolated and curvilinear regions of infrastructures and human bodies [7,12,14,15].

Self-powered flexible electronic systems are especially promising for *in vivo* biomedical applications since biological elements are composed of highly-cramped and totally isolated conditions. High performance flexible inorganic materials are capable of maintaining their functional properties in warm and humid environments [7,9,16,17]. In light of these aspects, human-integrated therapeutic and monitoring systems can be accomplished by the following approaches, schematically demonstrated in Figure 1. Fully-integrated flexible inorganic-based devices (*e.g.*, self-powered energy source, battery, processing integrated circuit (IC), LED, wireless communication, and antenna) can be conformally implanted and attached to a human body to cure diseases. A flexible energy harvester can generate electricity from the tiny biomechanical movement of human muscle to charge a flexible battery. The battery drives the main processing units (MPUs), LED-based sensor/stimulators and wireless communication modules for treatment of cardiac/brain disorders or the monitoring of vital signs such as blood pressure, pulse rate, oxygen level, and body temperature.

Since the heart, diaphragm, and shoulders move consistently as long as a human is alive, this system can be permanently operated by the abundant biomechanical energy of these sources, without battery replacement, which is a painful and dangerous operation for senior patients [18,19]. The collected physiological information is subsequently transmitted to external devices like smartphones by wireless RF communication. *In vivo* self-healing devices such as self-powered cardiac pacemakers and phototherapy tools can be also incorporated through the use of artificial electric or optogenetic stimulation [19,20].

This review paper introduces a brief overview of elemental devices and breakthrough approaches for realizing self-powered flexible inorganic electronic systems, including concepts, materials, devices and technologies. Continuing progress in these areas will open a new era of flexible ubiquitous systems, providing novel solutions for urgent issues facing humankind, including safety, environment, and healthcare monitoring.

Piezoelectric energy harvesters

In our daily surroundings, mechanical energy is more accessible than solar or thermal energy, because it is not restricted by time, place, or weather [21]. These mechanical and vibrational sources can potentially enable practical applications, not only electronic devices but also diverse sensor networks [22,23]. Several strategies have been studied for converting mechanical energy, such as electromagnetic induction [24], electrostatic generation [25,26], triboelectric electrification [27], and piezoelectricity [21,28,29]. In particular, energy harvesting technologies using piezoelectric materials have attracted huge attention due to their ability to directly convert mechanical energy into electricity. A variety of piezoelectric devices (*e.g.*, actuators, sensors, *etc.*) have been already commercialized in integrated electronics. However, the brittleness of their bulky ceramic materials places fundamental limitations on flexible applications, and produces low compatibility with curvilinear surfaces and poor responsiveness to tiny motions [22].

Flexible piezoelectric energy harvester, called nanogenerator (NG), can provide excellent energy conversion due to its high flexibility, light weight, and compatibility with plastic substrates [2,19,30–32]. Although the operating power required for high-end consumer electronics is still about 10 times higher than current nanogenerator technology (a few mW, Figure 2) [21], it is noteworthy that a self-powered cardiac pacemaker and several commercial electronic devices have been successfully operated with instantaneous responses to the minute strain produced by the slight bending motions of flexible substrates [19,32,33].

Nanoscale bottom-up piezoelectric materials have received enormous interests because they can achieve high electromechanical coupling from flexible biomechanical energy. Wang et al. have reported the observation of strain-induced voltage generation in vertically aligned ZnO

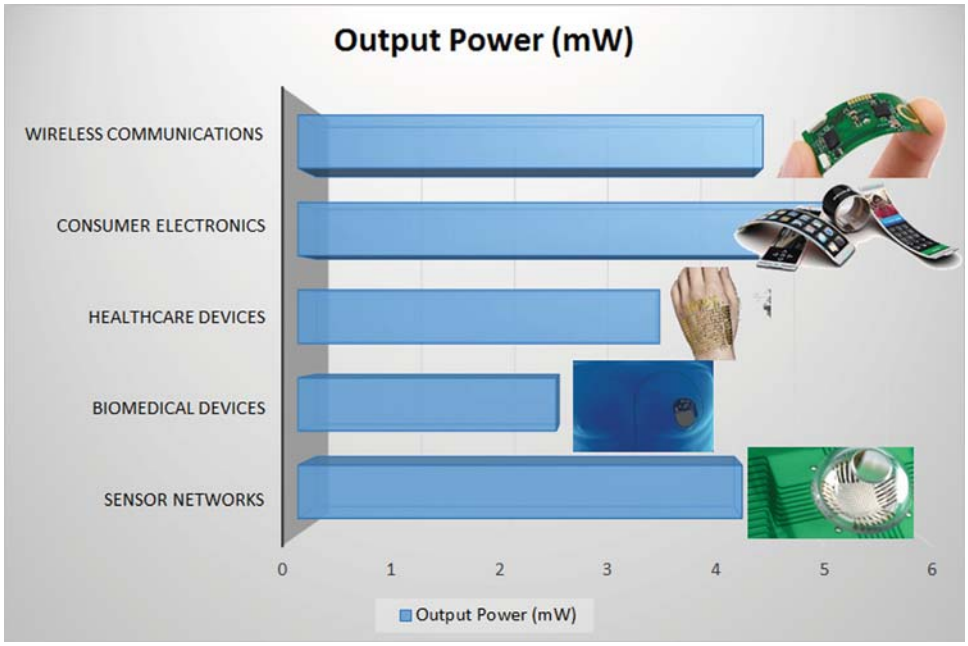

Figure 2 Power consumption of consumer electronics.

piezoelectric nanowires (NWs) on a GaN/sapphire substrate, using atomic force microscopy (AFM), as illustrated in Figure 3a [1]. When a constant force of 5 nN from the AFM contact mode was applied to the top of the ZnO NWs (Figure 3b), a sharp output voltage was observed for each corresponding contact position. A delay phenomenon was observed in the voltage signals in an analysis of the topographical map and the potential distribution of NWs (Figure 3c). Recently, Wang and coworkers significantly improved the performance of the flexible energy harvester using densely grown ZnO NW arrays on a plastic substrate, fabricated by a low temperature growth method (Figure 3d) [29,34]. The output voltage and current were up to 10 V and 600 nA at a strain of 0.12% and a strain rate of 3.56% s^{-1} (power density of 10 mW m^{-3}), sufficient to operate CMOS-based wireless communication for signal transmission at a distance of 5–10 m (Figure 3e) [21,34].

Flexible thin film energy harvesters

Perovskite crystal structured materials are exceedingly efficient and reliable for piezoelectric energy harvesting devices due to their high electromechanical coupling coefficient (d_{33}). For instance, $BaTiO_3$ (BTO), $PbZr_xTi_{1-x}O_3$ (PZT) and $Pb(Mg_{1/3}Nb_{2/3})O_3$-$PbTiO_3$ (PMN-PT) perovskite materials exhibit 3, 25 and 90 times higher d_{33} values compared to wurtzite ZnO materials, respectively [35]. PZT and BTO cantilever-type generators stimulated at resonance frequencies could realize an energy conversion efficiency above 80% [23]. However, general piezoelectric ceramics are brittle and bulky with limited capacity for flexible deformation. Although several efforts have been made to develop NWs-based perovskite nanogenerators, bottom-up approaches have the drawbacks of difficult synthesis and low performance [36–39].

Park et al. demonstrated an eco-friendly flexible BTO thin film energy harvester using the soft lithographic transfer of well-crystallized perovskite materials [2]. Note that these printing techniques overcome the thermal incompatibility between high temperature processes and plastic substrates, by transferring piezoelectric thin films which have been previously crystallized by 700 °C annealing on Si sacrificial substrates. Since it is essential to obtain crystallized and high quality perovskite materials for excellent energy conversion, the printing method is an optimal approach for a flexible nanogenerator [40,41]. However, the output performance of the BTO thin film nanogenerator (voltage of ~1.0 V and current of ~26 nA) was not sufficient to operate commercial electronics. This was due to the narrow horizontal length of the piezoelectric active regions, inevitably resulting from the wet etching of the sacrificial layer.

To overcome the size limitation of piezoelectric thin film on plastics, Hwang et al. developed a Ni film induced exfoliation strategy for transferring the entire area (1.7 cm × 1.7 cm) of a single crystalline PMN-PT film onto a flexible substrate [19]. The PMN-PT thin film energy harvester was able to scavenge tiny biomechanical bending motions to generate electricity with high output current of up to 0.223 mA and voltage of 8.2 V. This result illustrates how having a sufficient piezoactive area is extremely crucial for high performance flexible energy harvesting. The PMN-PT nanogenerator not only charged a coin cell battery, but also stimulated a living rat's heart as a self-powered cardiac pacemaker (Figure 4a). Figure 4b presents the animal experiment, with surgery on a rat's thorax, for stimulating the heart by regulating the heartbeat. Using the output current signals generated during bending/unbending motions (inset of Figure 4b and Figure 4c), the corresponding sharp pulses of the PMN-PT energy harvester clearly stimulated the rat's original heartbeat, as indicated by the electrocardiogram (ECG), shown in Figure 4d.

A high performance PZT thin film nanogenerator using an inorganic-based laser lift-off (ILLO) method was also introduced, combined with a cost-effective sol–gel thin film process [32]. The wafer-scale PZT thin film, crystallized at

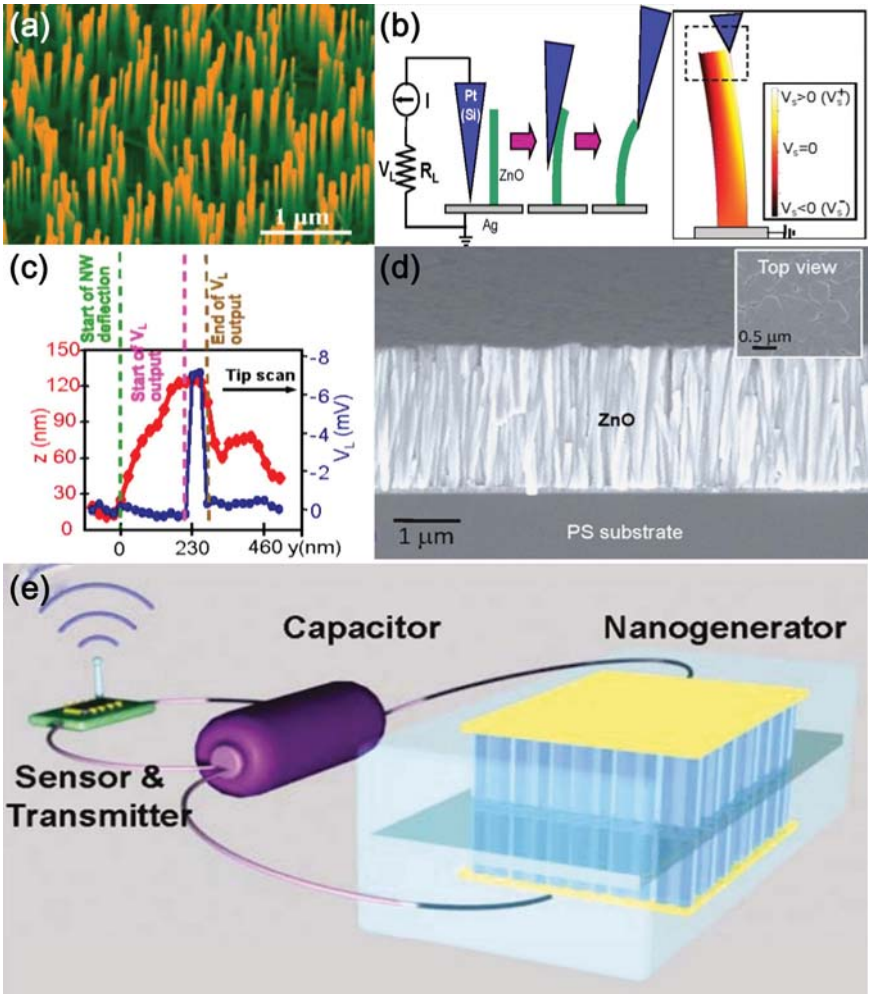

Figure 3 (a) SEM image of vertically aligned ZnO NWs grown on a GaN/sapphire wafer. (b) Electricity generation by the deformation of a piezoelectric ZnO NW using the direct contact of conductive AFM tip, which scans across the NWs. (c) The plots of the topology of ZnO NW arrays (red line) and the corresponding generated piezopotential (blue line) measured by the AFM analyses. (d) Cross-sectional SEM image of the densely grown NW textured film on the polystyrene (PS) substrate. The inset is the top view of the NW film. (e) A prototype schematic of an assembled self-powered system using a piezoelectric nanogenerator for mechanical energy harvesting. (a–c) Reproduced with permission from [1]. Copyright 2006, Science (AAAS). (d,e) Reprinted with permission from [34]. Copyright 2011, American Chemical Society.

650 °C, was then transferred from a bulk sapphire wafer to a flexible substrate by backside irradiation with an excimer laser. An image of the flexible PZT thin film nanogenerator with interdigitate electrodes (IDEs) is shown in Figure 4e. During periodic deformation of the PZT thin film energy harvester (3.5 cm × 3.5 cm), the output voltage and current reached up to ~250 V and 8.7 μA, respectively, the highest generated voltage among previously reported flexible piezoelectric nanogenerators. This flexible energy harvester was able to directly turn on over 100 blue LED bulbs without any external energy source (Figure 4f). The detailed mechanism and procedure of the ILLO process will be described in a later part of this review paper.

Nanocomposite generators

In 2012, Park et al. demonstrated a nanocomposite generator (NCG) fabricated by mixing piezoelectric BTO nanoparticles (NPs) and graphitic carbon (carbon nanotubes (CNTs) or reduced graphene oxide) with a polydimethylsiloxane (PDMS) matrix (Figure 5a) [30]. This nanocomposite-based piezoelectric generator can provide unique advantages, enabling cost-effective and large-area infrastructural applications, by excluding the vacuum chamber required by standard semiconductor processes. In the NCG devices, the CNTs or other conductive nanomaterials act as physically dispersing and mechanically reinforcing agents for effective piezopotential distribution and power generation [18,30,42]. Another important feature of the graphitic carbon is its role as an 'electrical nanobridge', providing conduction paths to reduce the internal resistance of the piezoelectric nanocomposite (p-NC) layer. The piezopotential produced by mechanical deformation vanished in the RC discharging process with a time constant (τ), as in the following Eq. (1),

$$\tau = (R_N + R_L) \times C_N \quad (1)$$

where R_N, R_L, and C_N are the internal resistance of p-NC, the load resistance of circuit, and the capacitance of p-NC,

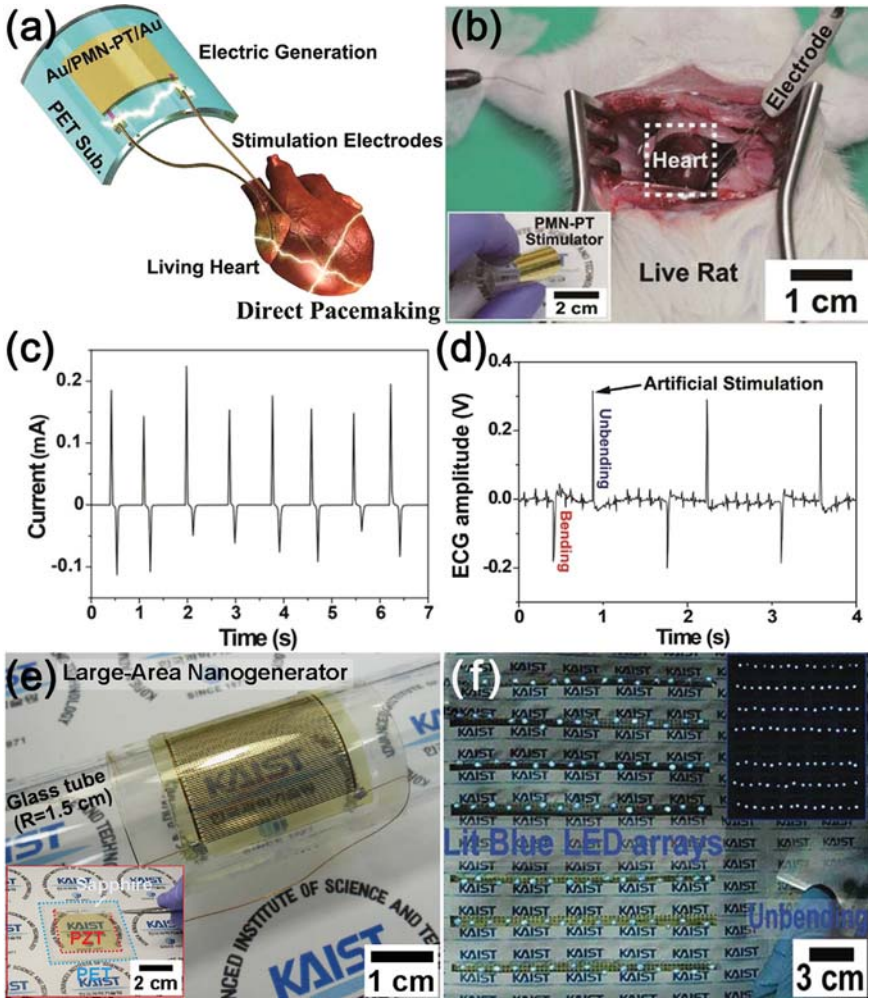

Figure 4 (a) Illustration figures of a fabricated flexible PMN-PT piezoelectric energy harvester and its biomedical application for cardiac pacemaking. (b) Digital photograph of the surgery experiment on an alive rat for the stimulation of the heart. The insert is a photo of flexible PMN-PT thin film stimulator used in the experiment. (c) Output short-circuit current from the flexible PMN-PT thin film energy harvester by finger flicking. (d) Considerable artificial peaks of the rat's ECG caused by the stimuli using the flexible PMN-PT energy harvester. (e) A large-area PZT thin film energy harvester (3.5 cm × 3.5 cm) on a glass cylinder (a radius of 1.5 cm). The inset presents a transferred large-area PZT thin film on a PET substrate from a sapphire wafer by the LLO method. (f) A captured photograph showing the turned on 105 blue LED bulbs in serial connection by the generated electrical energy from the PZT thin film energy harvester. The inset presents the operated LEDs in a darkroom. Reproduced with permission from [19,32]. Copyright 2014, John Wiley and Sons.

respectively. Therefore, the low internal resistance can result in a short lifetime which leads to the increasing amplitude of output voltage peaks [30,43].

To further enhance the output performance of the NCG, there have been several efforts to replace the piezoelectric particles with materials having higher piezoelectric coefficients, such as PZT and alkaline niobate particles [18,42]. Large-area NCG devices (30 cm × 30 cm) could be fabricated by bar/roller-coating or doctor-blade methods, as shown in Figure 5b. A large-scale NCG, stimulated by hand slapping, generated output voltage of above 140 V and current of about 10 μA, directly operating commercial red-green-blue (RGB) LED bulbs in serial connection.

Kim et al. reported unidirectional high-output generation using a composite-type hybrid piezoelectric nanogenerator based on $ZnSnO_3$ nanocube particles without carbon nanomaterials [44]. Under a rolling automobile tire, the nanogenerator successfully converted the car movement into electrical energy with voltage of ~20 V and current density of ~1 μA cm^{-2} (Figure 5c). Highly aligned and dense PZT nanofiber arrays fabricated by electrospinning were also assembled into a PDMS matrix to make a high-output nanogenerator, which was able to stimulate the sciatic nerve of a frog and induce the contraction of the gastrocnemius muscle [45]. Composite-based nanogenerators using 1D piezoelectric nanomaterials such as BTO, $KNbO_3$, $NaNbO_3$, and PMN-PT nanostructures have been also developed [46–50]. These 1D composite nanogenerators are highly attractive for large-scale energy harvesting applications because the 1D piezoelectric structures can be well dispersed in the polymeric matrix by themselves without additional dispersal agents like CNTs.

Jeong et al. introduced the 1D synthesis of bio-templated piezoelectric BTO nanomaterial for a flexible energy harvester, which was prepared by using the M13 virus as a

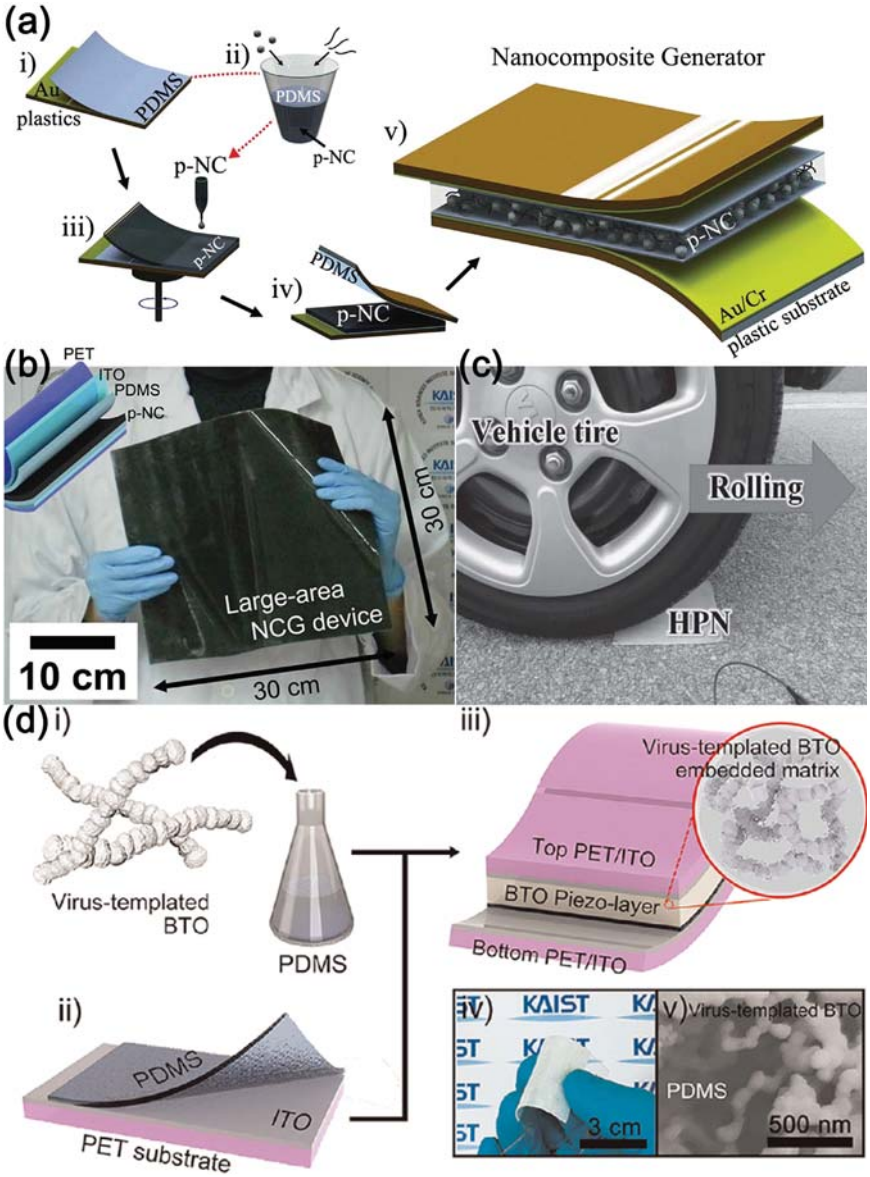

Figure 5 (a) Schemes of the fabrication for the NCG device composed of BTO NPs, CNTs, and PDMS matrix. (b) A photograph of the large-area NCG device (30 cm × 30 cm) fabricated by the Mayer bar-coating method. (c) The experimental setup for electricity generation using a composite-based nanogenerator under the rolling of an automobile wheel tire. Reproduced with permission from [30,42,44]. Copyright 2012, 2013, and 2014, John Wiley and Sons. (d) (i–iii) Schematic figures of the fabrication procedure for the virus-templated flexible nanogenerator. (iv) A digital photo of the nanogenerator and (v) an SEM image of well-entangled BTO nanostructures in the PDMS matrix. Reprinted with permission from [51]. Copyright 2013, American Chemical Society.

starting material [51]. The M13 virus was genetically modified to display triple glutamate groups (E3) on the outside of the p8 capsid protein. An intermediate virus-metal ion complex was utilized to prepare the virus-templated BTO 1D nanostructure. The filamentous form of the M13 virus resulted in the uniform dispersion of anisotropic piezoelectric BTO nanostructures, which is crucial for the generation of effective piezopotential. The bio-templated BTO nanostructures exhibiting high crystallinity and effective piezoelectricity were incorporated into an elastomeric matrix to fabricate a bio-inspired inorganic-based piezoelectric energy harvester (Figure 5d).

Flexible lithium ion batteries

Recently, the need for high performance flexible lithium ion batteries (f-LIBs) has dramatically increased as flexible displays come close to commercialization for future mobile electronics [52]. The key requirements for flexible batteries are high energy density, charge rate, stability, and durability [53–56]. However, the electric capacity of f-LIBs is still immature to operate wearable/flexible applications because of much thinner active areas compared to conventional massive LIBs which are generally composed of carbon-based anodes, lithium oxide-based cathodes, polymer separators,

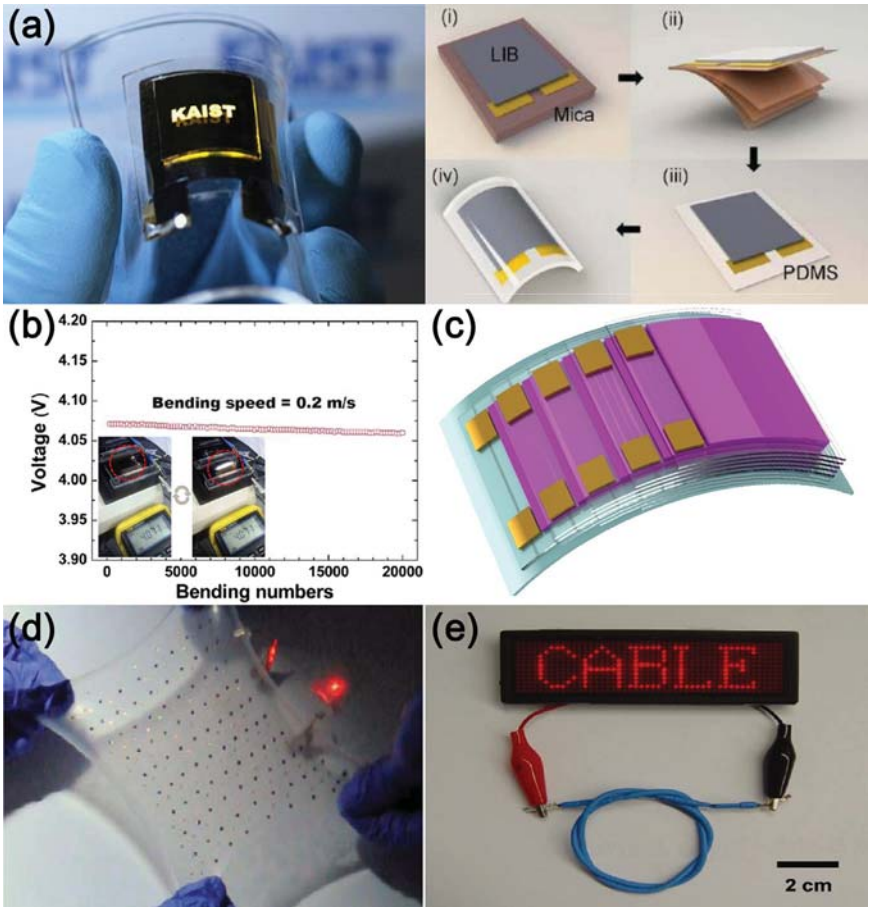

Figure 6 (a) Photograph of an all-flexible LED system operated by a flexible LIB, and schematic diagram of fabrication steps for the flexible LIB: (i) high temperature deposition process of LIB layers on a mica substrate, (ii) delamination of the mica substrate using adhesive tape, (iii) transfer of thin active layers onto a PDMS substrate, (iv) encapsulation with another PDMS layer for mechanical stability. (b) Voltage retentions test during 20,000 bending cycles. Inset: flat (left) and bent (right) state of the flexible thin film LIB. Reprinted with permission from [3]. Copyright 2012, American Chemical Society. (c) A conceptive image of multi-stacked thin film LIBs. (d) Operation of stretchable battery in biaxially stretched state. Reproduced with permission from [61]. Copyright 2013, Nature Publishing Group. (e) A picture of cable type LIB with excellent mechanical durability. Reproduced with permission from [62]. Copyright 2012, John Wiley and Sons.

and carbonate-based organic liquids as the electrolyte [57]. This traditional configuration of LIBs lacks mechanical flexibility, mainly due to the materials themselves: the rigid nature of ceramics, poor interconnection of active components, and unstable performance in flexible deformations [58].

The major innovations in f-LIBs are related to the development of materials and device structures, thus it is critical to consider the selection of high quality flexible electrodes [59,60]. Gwon et al. introduced carbon-based electrode materials based on multi-functional graphene papers [4]. Graphene oxide was dispersed by vacuum filtration on a 2 μm thick paper, and showed conductivity of ~8000 S m^{-1} with mechanical flexibility. In addition, the modulation of V_2O_5 deposition or pre-lithiation was shown to change the electrode polarity of the graphene papers, for applications as either a cathode or an anode.

Despite enormous research efforts focused on unit electrodes, the full-cell packaging of f-LIBs is still at a preliminary stage. Koo et al. demonstrated the first full-cell flexible thin film LIBs and its application for an all-in-one flexible electronic system (Figure 6a) [3]. All-solid-state thin film LIBs were constructed on a bulk mica substrate including lithium cobalt oxide cathode ($LiCoO_2$, crystallized at 700 °C), lithium phosphorous oxinitride (LiPON) electrolyte and lithium (Li) anode (Figure 6a-i). The sacrificial mica substrate was then removed by physical delamination, following weakening of the layered mica during high temperature annealing of the $LiCoO_2$ cathode electrode (Figure 6a-ii). After physical removal of the sacrificial substrates, the thin active battery layers were transferred onto flexible substrates (Figure 6a-iii) with another encapsulation layer (Figure 6a-iv) to settle the device on a neutral mechanical plane. The thin film f-LIBs exhibited high electrical performance (charging voltage of 4.2 V and capacity of 106 μAh cm^{-2}) and excellent durability after 20,000 bending cycles (Figure 6b). This approach will provide the multiple transfer of a multi-stacked thin film battery for high energy density (Figure 6c), which has previously been impossible because of material damage to the LiPON electrolyte caused by the subsequent high temperature processing of second layer $LiCoO_2$ cathodes.

Xu et al. have demonstrated novel strategies for stretchable LIBs using self-similar deformable interconnects [61]. These spring mechanics resulted in 300% biaxial stretchability of the

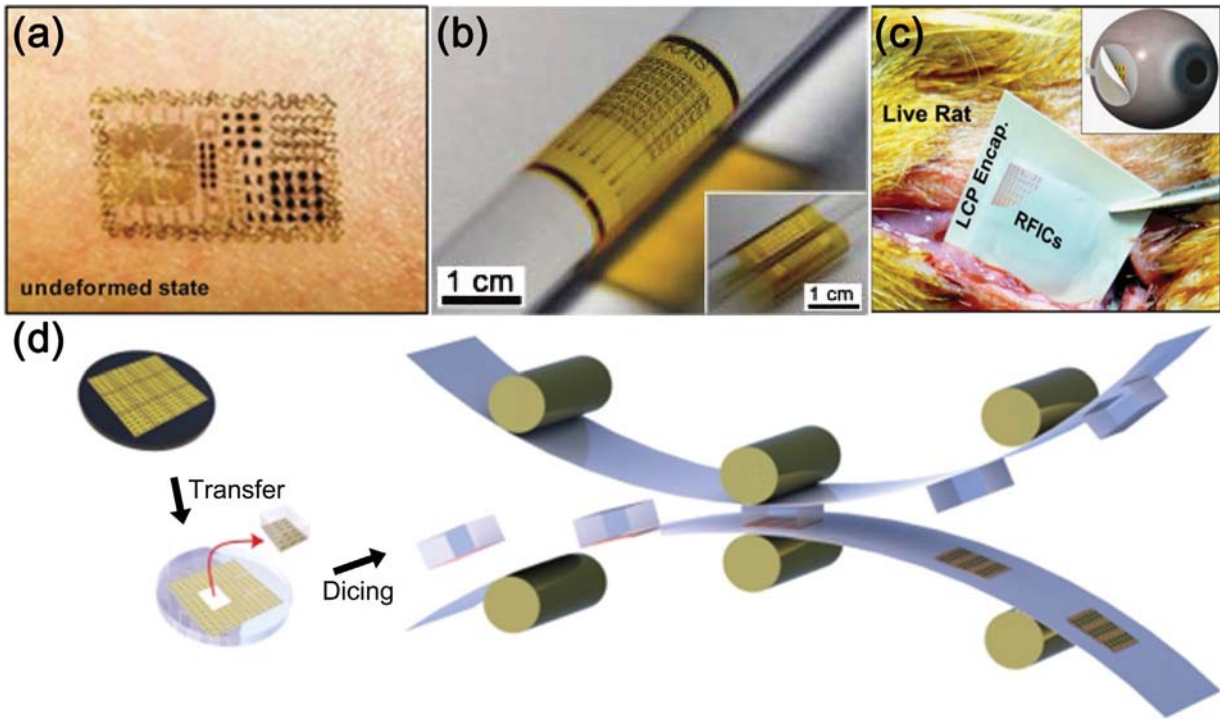

Figure 7 (a) Multifunctional sensors in intimate contact with epidermis. Reproduced with permission from [15]. Copyright 2011, Science (AAAS). (b) Photographs of the flexible logic memories conformally wrapped on a quartz rod and a bunch of two pipets (inset). Reprinted with permission from [5]. Copyright 2011, American Chemical Society. (c) A picture of biocompatible LSI implantation in a subcutaneous region, and a conceptual image of application on a sub-retinal area. Reprinted with permission from [7]. Copyright 2013, American Chemical Society. (d) Schemes of roll-to-roll process for large-scale transfer of electronics.

LIB, with the device showing a capacity of 1.1 mAh cm^{-2} (Figure 6d). Twistable and bendable batteries based on a coaxial cable design were also introduced by Kwon et al. The hollow-helix anode supported a polyethylene terephthalate (PET) nonwoven separator, and a $LiCoO_2$-coated spiral shape aluminum wire [62]. After packaging in an external insulator, a liquid organic electrolyte layer was stably injected into the battery cell. The final cable-like full-cell LIB was able to operate under the large strain of twisting conditions (Figure 6e).

Flexible inorganic electronics

The flexibility of an electronic system is highly crucial to achieving an intimate and conformal integration with human interfaces [16]. One solution is to use organic electronic materials, which often have simple and cost-effective deposition on flexible substrates [63]. However, they have also shown relatively low performance (*e.g.*, mobility, durability, *etc.*) and sensitivity to humid conditions [64,65], which make them unsuitable for biocompatible *in vivo* devices and outdoor wearable electronics. Although nanomaterials formed by bottom-up growth directly on plastic substrates have shown tremendous advances, several issues still remain to be solved, such as inaccurate alignment and incompatibility with the standard fabrication processes of semiconductor industry [66–68].

Rogers and coworkers have developed top-down approaches for fabricating flexible single-crystalline semiconductor electronics using thin film transfer from bulk inorganic wafers [69–74]. Photolithography and subsequent wet etching procedures are used to define the lateral dimensions of semiconductor nanomembranes, which can then be transferred by printing techniques from the mother substrates. Many researchers have demonstrated flexible inorganic electronic devices such as transistors, photovoltaics and sensors for wearable [75], dissolvable [76] and epidermal electronics (Figure 7a) [15].

Kim et al. demonstrated fully-functional flexible resistive random access memory (RRAM) with one transistor-one memristor (1T–1M) structures using a single-crystal silicon switcher and amorphous titanium oxide [5]. Using flexible 8×8 nonvolatile memory arrays on plastic substrates, the first random access operation on plastics was successfully measured to prove there was no electrical interference between adjacent cells. The flexible 1T-1M structure with ultrathin Si switcher, which can be conformally attached on curved surfaces (Figure 7b), will be a crucial architecture for fully-functional flexible memory for data processing, wireless communication, and information storage.

One drawback of the above-mentioned flexible inorganic electronics is the small number of possible transistor integrations, which hampers the realization of core logic processors and high-density memories. The main problem is related to the limited size of the active layer ($\sim$100 μm of horizontal length) and its nanoscale alignment on plastic substrates [77]. Hwang et al. reported flexible large-scale integration (LSI, thousands of nano-transistor integrations) based on the 0.18 RF CMOS process for implantable wireless communication [7]. The entire freestanding ultrathin LSI, composed of a 145 nm thick Si nanomembrane, was transferred from silicon on insulator (SOI) wafer onto a flexible

Table 1 Comparison of mechanical properties between LCP and other polymer substrates. Reproduced with permission from [9]. Copyright 2011, Elsevier.

	LCP	PI	PET
T_g (°C)	285	300	75
Water absorption (%)	0.04	2.9	0.5
Dielectric constant (at 1 MHz)	3.0	3.1	3.0
Oxygen transmission ($cm^3\ m^{-2}\ day^{-1}$, at 20-23 °C)	0.03-0.09	0.04-17	1.7-7.7
Water vapor transmission ($g\ m^{-2}\ day^{-1}$, at 37.8-40 °C)	0.006-0.016	0.4-21	3.9-17
Thermal expansion (ppm $°C^{-1}$)	0-30 controllable	20	15

liquid crystal polymer (LCP) and *in vivo* measurements of biocompatible f-LSI with LCP monolithic encapsulation were performed in live rats. Here, LCP is a promising biocompatible flexible material for implantable *in vivo* electronic applications given its mechanical stability, chemical resistance, low water absorption, high temperature durability, excellent dielectric property, and low thermal expansion compared to other commercialized flexible substrates such as PET and polyimide (PI) substrate (Table 1) [9]. Moreover, monolithic packaging of LCP can totally block the penetration of ions and moisture while providing small, light, and cost-efficient advantages over conventional biomedical packaging using ceramics and titanium materials [78]. This advanced monolithic packaging of semiconductor devices facilitates stable and durable operation of f-LSI in solution-based biointegrated conditions (Figure 7c). Roll-to-roll printing process can be also applied (Figure 7d) for commercial flexible logic products including display drivers, smart watches, and retinal prosthesis.

Flexible inorganic optoelectronics

Flexible optoelectronics play a significant role in displays, communication, sensors and biomedical stimulators. Flexible organic LEDs (OLEDs) have been intensively studied for the last two decades due to their easy fabrication and compatibility with polymeric substrates [79,80]. Despite the big success of OLEDs in the display industry, OLEDs still have disadvantages in efficiency, brightness, lifetime and instability in humid conditions, which are especially significant for *in vivo* bio-applications [9,17,81]. On the contrary, inorganic light-emitting diodes (ILEDs) are promising solid-state light sources with excellent electrical, optical and mechanical properties [82,83]. LEDs are widely commercialized and used in daily life as light sources [84], back light units (BLUs) for displays [85], biosensors [86] and therapeutic tools [87]. Although flexible ILEDs (f-ILEDs) are difficult to achieve due to the brittle nature of inorganic materials, this technology can have high impact on both industrial and research communities in the fields of flexible light source and biomedical applications.

Recent advances in the transfer of inorganic thin films have advanced the development of reliable and high performance f-ILEDs on plastic substrates [6,88-90]. Lee et al. demonstrated water-resistant flexible blue LEDs on a biocompatible LCP substrate (Figure 8a) [9]. Starting with the epitaxial growth of GaN LED layers on a silicon substrate, a high temperature (600-900 °C) ohmic contact was then formed on both n- and p-type GaN. The free-standing inorganic LEDs were then transferred onto a flexible LCP substrate by selective etching of sacrificial silicon wafer. The resulting flexible GaN LEDs with polytetrafluoroethylene (PTFE) passivation showed superb optical power, water resistance and biocompatibility, leading to an interesting prototype of a prostate-specific antigen biosensor with a detection limit of 1 ng mL^{-1}.

A flexible red inorganic LED is also important for photodynamic therapies and biosensors. Park et al. reported flexible AlInGaP ILEDs on elastomeric substrates (Figure 8b) after a selective removal of a sacrificial AlGaAs layer [10]. Nevertheless, as described previously, selective wet etching of the sacrificial interlayer inevitably results in size limitation, along with the high cost of growing epitaxial LED layers on unusual interlayer.

Recently, a facile approach of fabricating high performance flexible vertical structure LEDs (f-VLEDs) was demonstrated using anisotropic conductive film (ACF) bonding (Figure 8c-i) and removal of the entire GaAs mother wafer (Figure 8c-ii) [14]. This approach can overcome the size limitations and cost issue of the interlayer wet etching process by using widely commercialized GaAs product. The characteristics of the f-VLEDs were stably maintained in a bending state with a radius of 3 mm over 1000 bending cycles. In addition, the red f-VLEDs were operated using a flexible PZT piezoelectric energy harvester as a self-powered energy source (Figure 8d). The schematic image in Figure 8e shows that the f-ILED surrounds a blood vessel, for use as an implantable and label-free biosensor.

Inorganic-based laser lift-off (ILLO) for flexible applications

Flexible electronics using single crystalline inorganic semiconductors have shown unprecedented potential for performance enhancement and reliability. However, as noted earlier, the printing transfer technology has several drawbacks related to the complicated wet etching procedure, leading to restricted dimension, high cost, and low throughput [77]. Thus the large-area applications such as displays and touch panels may not be accomplished using the printing method. One solution for large-area flexible applications utilizes the beneficial properties of laser material interactions; the laser's narrow wavelength and extremely short duration (~ tens of ns) facilitates spatial-temporal laser annealing on various substrates [91,92]. For instance, the high temperature crystallization of amorphous Si (above 1000 °C) directly on plastic substrates using excimer laser

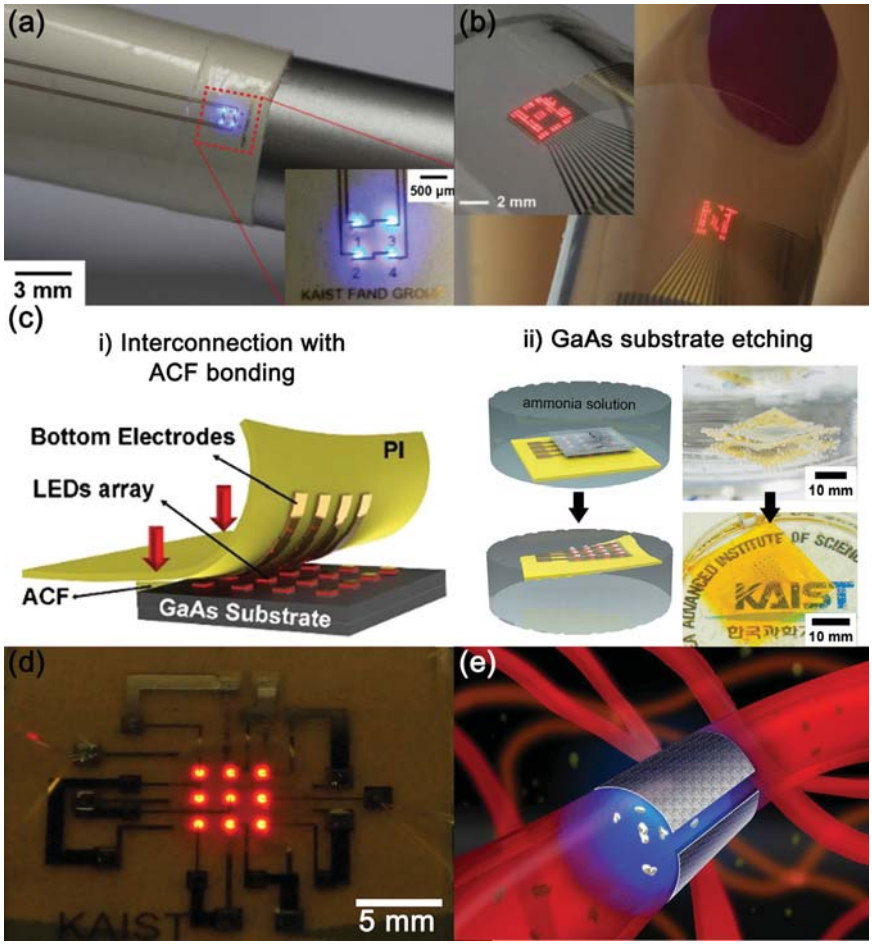

Figure 8 (a) Images of 2×2 GaN LEDs on an LCP substrate and the magnified photograph (inset). Reproduced with permission from [9]. Copyright 2011, Elsevier. (b) Flexible passive matrix display consisting of 16×16 array AlInGaP LEDs on a plastic substrate covering around the curvilinear surfaces of a dummy hand and a glass tube (inset). Reproduced with permission from [10]. Copyright 2009, Science (AAAS). (c) (i) The ACF bonding of AlGaInP red LEDs to a plastic substrate. (ii) GaAs wafer with LED chips bonded on a plastic substrate by the ACF sinks into the specific ammonia-based etchant. The GaAs mother substrate is completely removed after about 1 h. The f-VLEDs array spontaneously floats on the surface of the etchant solution. (d) Digital photograph of a 3×3 array of flexible red LEDs made by the method (c). Reproduced with permission from [18]. Copyright 2014, Royal Society of Chemistry. (e) A schematic image of implantable flexible inorganic LEDs for label-free biosensing. Reproduced with permission from [16]. Copyright 2012, Dove Press.

enables the low temperature polysilicon (LTPS, electron mobility of 190 $cm^2 V^{-1} s^{-1}$) process of AMOLED active matrix [93].

The dry transfer method, inorganic-based laser lift-off (ILLO), has also been developed as a promising methodology to manufacture large-area flexible inorganic devices without using a wet etching process. The excimer laser can successfully transfer high performance inorganic thin films onto plastics from transparent bulk substrates with excellent reproducibility, productivity, and compatibility with the current production line of the display industry [94]. High-quality inorganic-based flexible electronics, such as LEDs [95], high-density memories [96], and energy devices [32], can be realized by laser interfacial irradiation between a transparent mother substrate and laser-reactive sacrificial layer. Several groups have demonstrated the fabrication of flexible GaN LEDs using LLO by melting the interface between a GaN and a sapphire wafer [97,98]. As with the flexible GaN LEDs transferred from a Si substrate, high-quality epitaxial LED can be transferred onto a flexible substrate. The key issue of GaN ILLO is related to the management of induced destructive stresses produced by the decomposition of the sacrificial layer. A supporting adhesion layer can release this stress and safely hold the resulting freestanding inorganic GaN on a flexible substrate (Figure 9a) [95].

Park et al. introduced a high performance flexible PZT thin film energy harvester using ILLO of sol-gel PZT layers [32]. The XeCl excimer laser beam was exposed to the backside of the sapphire substrate to separate the entire area (3.5 cm × 3.5 cm) of the PZT layer to be directly attached onto a PET film (Figure 9b). The photonic energy of the XeCl laser (4.03 eV) is smaller than the band gap energy of sapphire (8.7 eV) and larger than that of PZT (3.2-3.6 eV) so that the laser beam penetrates the sapphire wafer, causing the partial melting and decomposition of PZT at the interface with the sapphire wafer.

Kim et al. demonstrated the ILLO approach for high-density crossbar-structured flexible memory arrays employing a laser-reactive exfoliation layer [96]. High-density crossbar-structured RRAM arrays of one selector-one resistor (1S-1R) were

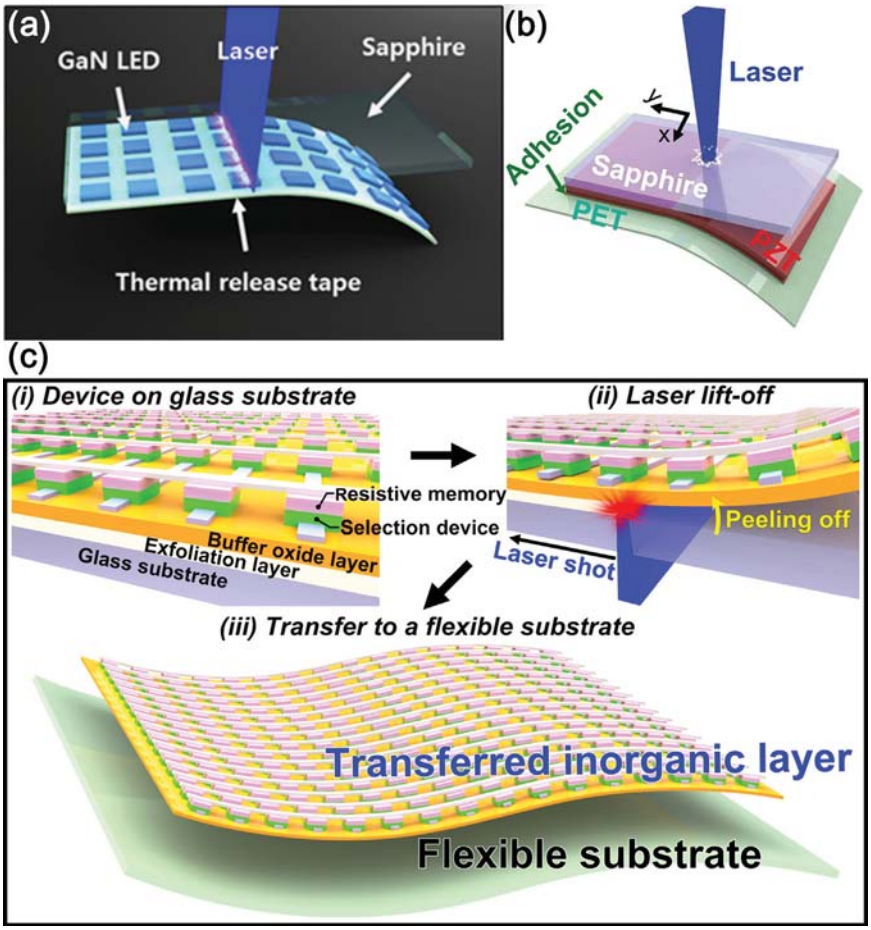

Figure 9 (a) Illustration of LLO separation of GaN LED chips from the sapphire substrate. (b) A schematic image of LLO of PZT thin film. (c) Graphical drawings of the fabrication process of crossbar-structured flexible memory arrays utilizing the LLO method. Reproduced with permission from [32,96]. Copyright 2014, John Wiley and Sons.

fabricated on a rigid glass substrate consisting of an amorphous silicon (a-Si:H) sacrificial layer, Ni/TiO_2/Ni selector and Pt/NiO_x/Ni resistor (Figure 9a-i). A 308 nm excimer laser was irradiated from the backside of the glass substrate and melted out the a-Si:H layer, thus detaching only the top 500 nm-thick active memory layers from the mother glass substrate (Figure 9a-ii). To avoid the fracture of active memories during ILLO, an epoxy encapsulation layer and a thermal release tape were used to hold the device layers. The large-size active 1S-1R RRAM were then transferred to a plastic substrate (Figure 9a-iii). Due to its high reliability, this novel idea may be extended to the next-generation large-area applications (*Gen 10*, 2.88 m $\times$ 3.13 m) such as active matrix of display and thin film inorganic solar cell, which can be combined with roll-to-roll mass production.

Self-powered flexible electronic systems

The concept of self-powered fully-flexible electronic systems has been a dream of both medical and electronic scientists because they can scavenge biomechanical energy and facilitate intimate contact on curvilinear organs [21,99]. Such biomedical devices can be placed in completely-isolated *in vivo* conditions where electrical energy cannot be supplied by external power sources. The ultimate solution is to utilize the abundant mechanical energy sources existing in the human body [33]. Although it is not yet possible to make all electronic and energy devices flexible on a single plastic substrate, diverse types of flexible energy harvesters have been studied for wearable electronics [100-103].

Flexible thermoelectric power generator is a potential candidate for providing sustainable energy for wearable electronics, because of the consistent temperature gradient between humans and ambient conditions. Kim et al. reported a wearable thermoelectric generator using a screen printing method on glass fabric [104]. The output power density reached a higher value (28 mW g^{-1} at ΔT=50 K) than previously reported thermoelectric devices, and achieved a bandage application on a human wrist. However, the temperature gradient around the human body is generally not enough to generate sufficient electricity for driving practical consumer devices. Triboelectric energy harvester based on the coupling of frictional electrification and electrostatic induction can generate huge power, sufficient to even drive a mobile phone. Jung et al. demonstrated a wearable fabric-based triboelectric integrated energy generator [105]. This energy harvesting device with power density of 0.18 $\mu A\,cm^{-2}$ was able to monitor human activity and supply energy for operating external pressure sensors. Nonetheless, the relatively new

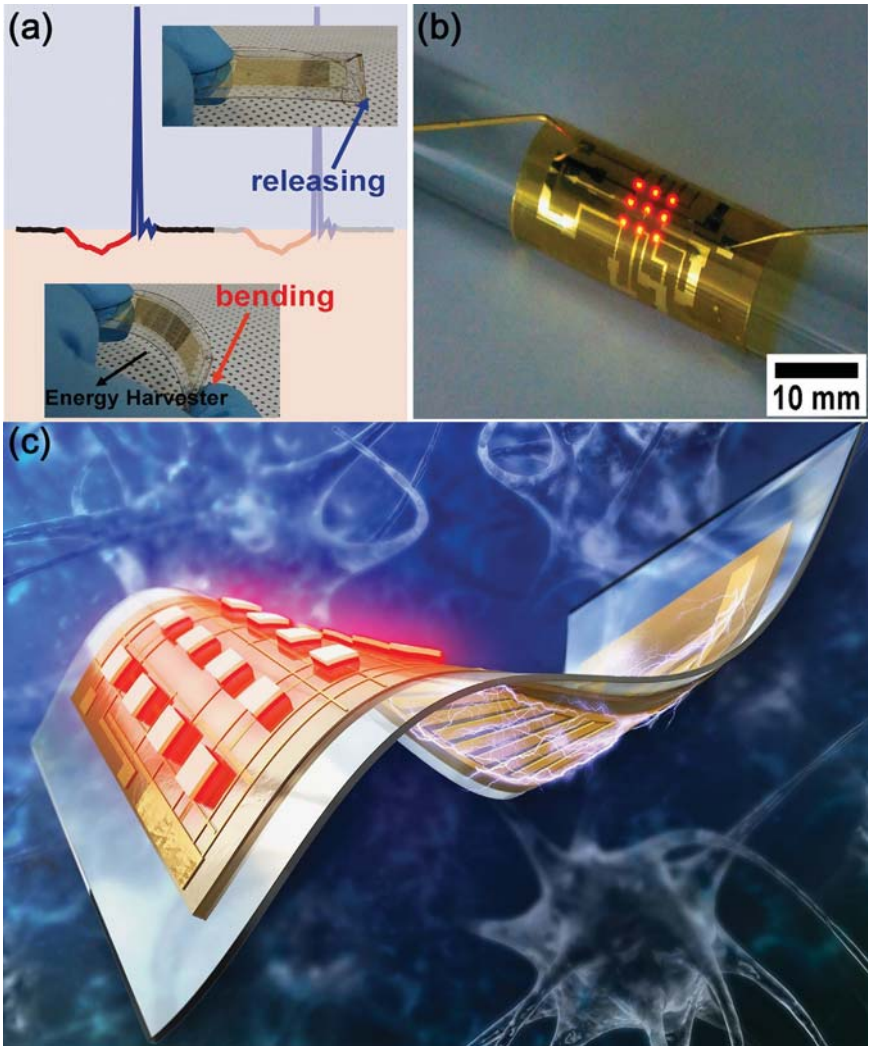

Figure 10 (a) Photographs of the flexible PZT energy harvester at bending/releasing states, and corresponding generated output current. (b) Photographs of a 3×3 array of operated f-VLEDs on a curved glass in the self-powered flexible light-emitting system. (c) Self-powered fully-flexible light-emitting system on single flexible substrate will be applied to various biomedical purposes such as phototherapy and optogenetics. Reproduced with permission from [14]. Copyright 2014, Royal Society of Chemistry.

field of triboelectric technology has to focus on extensive research to address limitations that affect friction phenomenon, such as humidity, sensitivity, and abrasion resistance. Moreover, the triboelectric energy harvester is not perfectly suitable for flexible systems since two counterpart substrates cannot effectively respond to slight motions [106].

Jeong et al. successfully realized the first self-powered fully-flexible electronic system by combining a flexible piezoelectric energy harvester and flexible VLED optoelectronics [14]. The flexible PZT thin film piezoelectric generator made by ILLO could operate the f-VLED devices during bending/releasing deformations driven by finger movements (Figure 10a). The flexible piezoelectric energy harvester had output voltage and current of $\sim$140 V and $\sim$10 μA, which was sufficient to directly drive the flexible 3×3f-VLED array (Figure 10b) without any external energy supply. The paper also contains significant advances demonstrating that two different fields of high performance flexible inorganic devices can be integrated on plastic substrates by the sophisticated optimization of f-ILED and self-powered energy. Figure 10c depicts the conceptual image of a self-powered flexible optoelectronic system on a single plastic substrate for various biomedical applications.

Conclusion

The emergence of self-powered flexible electronic systems represents a great paradigm shift in future electronics for human-friendly or human-integrated fields. In particular, such systems are of immediate interest for application in sensor networks and wearable electronics by accessing permanent energy sources, and delivering power harvested from abundant mechanical energy. Novel flexible systems include combinations of flexible energy harvesters, batteries, LEDs, sensors, high-density memories, and LSI on a single plastic substrates. The key issue today lies in how to obtain large-scale and high performance flexible inorganic thin films. Laser-assisted processes such as inorganic-based laser lift-off and high temperature annealing directly on

plastics will become more and more important in the future flexible era. Finally, self-powered fully-flexible electronic systems will open up unprecedented *in vivo* biomedical applications (*e.g.*, self-powered cardiac pacemaker, implantable biosensor, phototherapeutic or optogenetic tools) [107]. These innovations are strongly related to the development of material advancements, processing strategies, and device integration, which requires the interdisciplinary research of IT, biotechnology (BT), nanotechnology (NT), and environment technology (ET).

Acknowledgment

This work was supported by the Basic Science Research Program (Grant code: NRF-2012R1A2A1A03010415), Center for Integrated Smart Sensors as Global Frontier Project (CISS-2012M3A6A6054193) funded by the Korea Government (MSIP) through the National Research Foundation of Korea (NRF).

References

[1] Z.L. Wang, J. Song, Science 312 (2006) 242–246.
[2] K.-I. Park, S. Xu, Y. Liu, G.-T. Hwang, S.-J.L. Kang, Z.L. Wang, K.J. Lee, Nano Lett. 10 (2010) 4939–4943.
[3] M. Koo, K.-I. Park, S.H. Lee, M. Suh, D.Y. Jeon, J.W. Choi, K. Kang, K.J. Lee, Nano Lett. 12 (2012) 4810–4816.
[4] H. Gwon, H.-S. Kim, K.U. Lee, D.-H. Seo, Y.C. Park, Y.-S. Lee, B.T. Ahn, K. Kang, Energy Environ. Sci. 4 (2011) 1277–1283.
[5] S. Kim, H.Y. Jeong, S.K. Kim, S.-Y. Choi, K.J. Lee, Nano Lett. 11 (2011) 5438–5442.
[6] J.-H. Ahn, H.-S. Kim, K.J. Lee, S. Jeon, S.J. Kang, Y. Sun, R.G. Nuzzo, J.A. Rogers, Science 314 (2006) 1754–1757.
[7] G.-T. Hwang, D. Im, S.E. Lee, J. Lee, M. Koo, S.Y. Park, S. Kim, K. Yang, S.J. Kim, K. Lee, K.J. Lee, ACS Nano 7 (2013) 4545–4553.
[8] Y. Zhai, L. Mathew, R. Rao, D. Xu, S.K. Banerjee, Nano Lett. 12 (2012) 5609–5615.
[9] S.Y. Lee, K.-I. Park, C. Huh, M. Koo, H.G. Yoo, S. Kim, C.S. Ah, G.Y. Sung, K.J. Lee, Nano Energy 1 (2012) 145–151.
[10] S.-I. Park, Y. Xiong, R.-H. Kim, P. Elvikis, M. Meitl, D.-H. Kim, J. Wu, J. Yoon, C.-J. Yu, Z. Liu, Y. Huang, K. Hwang, P. Ferreira, X. Li, K. Choquette, J.A. Rogers, Science 325 (2009) 977–981.
[11] J. Zhou, Y. Gu, P. Fei, W. Mai, Y. Gao, R. Yang, G. Bao, Z.L. Wang, Nano Lett. 8 (2008) 3035–3040.
[12] H.S. Lee, J. Chung, G.-T. Hwang, C.K. Jeong, Y. Jung, J.-H. Kwak, H. Kang, M. Byun, W.D. Kim, S. Hur, S.-H. Oh, K.J. Lee, Adv. Funct. Mater. 24 (2014) 6914–6921. http://dx.doi.org/10.1002/adfm.201402270.
[13] S. Jung, J.H. Kim, J. Kim, S. Choi, J. Lee, I. Park, T. Hyeon, D.-H. Kim, Adv. Mater. 26 (2014) 4825–4830.
[14] C.K. Jeong, K.-I. Park, J.H. Son, G.-T. Hwang, S.H. Lee, D.Y. Park, H.E. Lee, H.K. Lee, M. Byun, K.J. Lee, Energy Environ. Sci. 7 (2014) 4035–4043 http://dx.doi.org/10.1039/C4EE02435D.
[15] D.-H. Kim, N. Lu, R. Ma, Y.-S. Kim, R.-H. Kim, S. Wang, J. Wu, S.M. Won, H. Tao, A. Islam, K.J. Yu, T. Kim, R. Chowdhury, M. Ying, L. Xu, M. Li, H.-J. Chung, H. Keum, M. McCormick, P. Liu, Y.-W. Zhang, F.G. Omenetto, Y. Huang, T. Coleman, J.A. Rogers, Science 333 (2011) 838–843.
[16] M. Koo, S.Y. Park, K.J. Lee, Nanobiosensors Dis. Diagn. 1 (2012) 5–15.
[17] H.G. Yoo, K.-I. Park, M. Koo, S. Kim, S.Y. Lee, S.H. Lee, K.J. Lee, Proc. SPIE 8268 (2012) 82681Y.
[18] C.K. Jeong, K.-I. Park, J. Ryu, G.-T. Hwang, K.J. Lee, Adv. Funct. Mater. 24 (2014) 2620–2629.
[19] G.-T. Hwang, H. Park, J.H. Lee, S. Oh, K.-I. Park, M. Byun, H. Park, G. Ahn, C.K. Jeong, K. No, H. Kwon, S.G. Lee, B. Joung, K.J. Lee, Adv. Mater. 26 (2014) 4880–4887.
[20] T. Kim, J.G. McCall, Y.H. Jung, X. Huang, E.R. Siuda, Y. Li, J. Song, Y.M. Song, H.A. Pao, R.-H. Kim, C. Lu, S.D. Lee, I.-S. Song, G. Shin, R. Al-Hasani, S. Kim, M.P. Tan, Y. Huang, F.G. Omenetto, J.A. Rogers, M.R. Bruchas, Science 340 (2013) 211–216.
[21] Z.L. Wang, W. Wu, Angew. Chem. Int. Ed. Engl. 51 (2012) 11700–11721.
[22] Z.L. Wang, Adv. Funct. Mater. 18 (2008) 3553–3567.
[23] X. Wang, Nano Energy 1 (2012) 13–24.
[24] S.P. Beeby, R.N. Torah, M.J. Tudor, P. Glynne-Jones, T. O'Donnell, C.R. Saha, S. Roy, J. Micromechanics Microengineering 17 (2007) 1257–1265.
[25] R. Peirine, R. Kornbluh, J. Eckerle, P. Jeuck, S. Oh, Q. Pei, S. Stanford, Proc. SPIE 4329 (2001) 148–156.
[26] P.D. Mitcheson, P. Miao, B.H. Stark, E.M. Yeatman, A. S. Holmes, T.C. Green, Sens. Actuators, A Phys. (2004) 523–529.
[27] Z.L. Wang, ACS Nano 7 (2013) 9533–9557.
[28] Z.L. Wang, G. Zhu, Y. Yang, S. Wang, C. Pan, Mater. Today 15 (2012) 532–543.
[29] Z.L. Wang, Adv. Mater. 24 (2012) 280–285.
[30] K.-I. Park, M. Lee, Y. Liu, S. Moon, G.T. Hwang, G. Zhu, J.E. Kim, S.O. Kim, D.K. Kim, Z.L. Wang, K.J. Lee, Adv. Mater. 24 (2012) 2999–3004.
[31] S. Lee, S.H. Bae, L. Lin, Y. Yang, C. Park, S.W. Kim, S.N. Cha, H. Kim, Y.J. Park, Z.L. Wang, Adv. Funct. Mater. 23 (2013) 2445–2449.
[32] K.-I. Park, J.H. Son, G.-T. Hwang, C.K. Jeong, J. Ryu, M. Koo, I. Choi, S.H. Lee, M. Byun, Z.L. Wang, K.J. Lee, Adv. Mater. 26 (2014) 2514–2520.
[33] C. Dagdeviren, B.D. Yang, Y. Su, P.L. Tran, P. Joe, E. Anderson, J. Xia, V. Doraiswamy, B. Dehdashti, X. Feng, B. Lu, R. Poston, Z. Khalpey, R. Ghaffari, Y. Huang, M. J. Slepian, J.A. Rogers, Proc. Natl. Acad. Sci. USA 111 (2014) 1927–1932.
[34] Y. Hu, Y. Zhang, C. Xu, L. Lin, R.L. Snyder, Z.L. Wang, Nano Lett. 11 (2011) 2572–2577.
[35] I.R. Henderson, Piezoelectric Ceramics: Principles and Applications, APC International, Ltd., Mackeyville PA, 2002.
[36] S. Xu, B.J. Hansen, Z.L. Wang, Nat. Commun. 1 (2010) 93. http://dx.doi.org/10.1038/ncomms1098.
[37] A. Koka, H.A. Sodano, Nat. Commun. 4 (2013) 2682. http://dx.doi.org/10.1038/ncomms3682.
[38] A. Koka, Z. Zhou, H.A. Sodano, Energy Environ. Sci. 7 (2014) 288–296.
[39] A. Koka, H.A. Sodano, Adv. Energy Mater. 4 (2014) 1301660.
[40] Y. Qi, M.C. McAlpine, Energy Environ. Sci. 3 (2010) 1275.
[41] Y. Qi, J. Kim, T.D. Nguyen, B. Lisko, P.K. Purohit, M.C. McAlpine, Nano Lett. 11 (2011) 1331–1336.
[42] K.-I. Park, C.K. Jeong, J. Ryu, G.-T. Hwang, K.J. Lee, Adv. Energy Mater. 3 (2013) 1539–1544.
[43] H. Sun, H. Tian, Y. Yang, D. Xie, Y.C. Zhang, X. Liu, S. Ma, H.M. Zhao, T.L. Ren, Nanoscale 5 (2013) 6117–6123.
[44] K.Y. Lee, D. Kim, J.H. Lee, T.Y. Kim, M.K. Gupta, S.W. Kim, Adv. Funct. Mater. 24 (2014) 37–43.
[45] L. Gu, N. Cui, L. Cheng, Q. Xu, S. Bai, M. Yuan, W. Wu, J. Liu, Y. Zhao, F. Ma, Y. Qin, Z.L. Wang, Nano Lett. 13 (2013) 91–94.
[46] J.H. Jung, M. Lee, J. Il Hong, Y. Ding, C.Y. Chen, L.J. Chou, Z.L. Wang, ACS Nano 5 (2011) 10041–10046.
[47] J.H. Jung, C.-Y. Chen, B.K. Yun, N. Lee, Y. Zhou, W. Jo, L.-J. Chou, Z.L. Wang, Nanotechnology 23 (2012) 375401.
[48] Z.-H. Lin, Y. Yang, J.M. Wu, Y. Liu, F. Zhang, Z.L. Wang, J. Phys. Chem. Lett. 3 (2012) 3599–3604.

[49] S. Xu, Y.W. Yeh, G. Poirier, M.C. McAlpine, R.A. Register, N. Yao, Nano Lett. 13 (2013) 2393–2398.
[50] K.-I. Park, S. Bin Bae, S.H. Yang, H.I. Lee, K. Lee, S.J. Lee, Nanoscale 6 (2014) 8962–8968.
[51] C.K. Jeong, I. Kim, K.-I. Park, M.H. Oh, H. Paik, G.-T. Hwang, K. No, Y.S. Nam, K.J. Lee, ACS Nano 7 (2013) 11016–11025.
[52] H.G. Yoo, S. Kim, K.J. Lee, RSC Adv. 4 (2014) 20017–20023.
[53] B. Scrosati, Nature 373 (1995) 557–558.
[54] H. Nishide, K. Oyaizu, Science 319 (2008) 737–738.
[55] L. Hu, J.W. Choi, Y. Yang, S. Jeong, F. La Mantia, L.-F. Cui, Y. Cui, Proc. Natl. Acad. Sci. USA 106 (2009) 21490–21494.
[56] G. Jeong, Y.-U. Kim, H. Kim, Y.-J. Kim, H.-J. Sohn, Energy Environ. Sci. 4 (2011) 1986–2002.
[57] G. Zhou, F. Li, H.-M. Cheng, Energy Environ. Sci. 7 (2014) 1307–1338.
[58] H. Gwon, J. Hong, H. Kim, D.-H. Seo, S. Jeon, K. Kang, Energy Environ. Sci. 7 (2014) 538–551.
[59] S.W. Lee, N. Yabuuchi, B.M. Gallant, S. Chen, B.-S. Kim, P.T. Hammond, Y. Shao-Horn, Nat. Nanotechnol. 5 (2010) 531–537.
[60] R. Mukherjee, A.V. Thomas, A. Krishnamurthy, N. Koratkar, ACS Nano 6 (2012) 7867–7878.
[61] S. Xu, Y. Zhang, J. Cho, J. Lee, X. Huang, L. Jia, J.A Fan, Y. Su, J. Su, H. Zhang, H. Cheng, B. Lu, C. Yu, C. Chuang, T.-I. Kim, T. Song, K. Shigeta, S. Kang, C. Dagdeviren, I. Petrov, P.V Braun, Y. Huang, U. Paik, J.A. Rogers, Nat. Commun. 4 (2013) 1543. http://dx.doi.org/10.1038/ncomms2553.
[62] Y.H. Kwon, S.-W. Woo, H.-R. Jung, H.K. Yu, K. Kim, B.H. Oh, S. Ahn, S.-Y. Lee, S.-W. Song, J. Cho, H.-C. Shin, J.Y. Kim, Adv. Mater. 24 (2012) 5192–5197.
[63] M. Kaltenbrunner, T. Sekitani, J. Reeder, T. Yokota, K. Kuribara, T. Tokuhara, M. Drack, R. Schwödiauer, I. Graz, S. Bauer-Gogonea, S. Bauer, T. Someya, Nature 499 (2013) 458–463.
[64] K. Nomura, H. Ohta, A. Takagi, T. Kamiya, M. Hirano, H. Hosono, Nature 432 (2004) 488–492.
[65] J. Lewis, Mater. Today 9 (2006) 38–45.
[66] M.C. McAlpine, H. Ahmad, D. Wang, J.R. Heath, Nat. Mater. 6 (2007) 379–384.
[67] A. Manekkathodi, M.-Y. Lu, C.W. Wang, L.-J. Chen, Adv. Mater. 22 (2010) 4059–4063.
[68] K. Takei, T. Takahashi, J.C. Ho, H. Ko, A.G. Gillies, P.W. Leu, R.S. Fearing, A. Javey, Nat. Mater. 9 (2010) 821–826.
[69] J.H. Ahn, H.S. Kim, K.J. Lee, Z. Zhu, E. Menard, R.G. Nuzzo, J.A. Rogers, IEEE Electron Device Lett. 27 (2006) 460–462.
[70] D.-H. Kim, Z. Liu, Y.-S. Kim, J. Wu, J. Song, H.-S. Kim, Y. Huang, K.-C. Hwang, Y. Zhang, J.A. Rogers, Small 5 (2009) 2841–2847.
[71] K.J. Lee, H. Ahn, M.J. Motala, R.G. Nuzzo, E. Menard, J.A. Rogers, J. Micromechanics Microengineering 20 (2010) 075018.
[72] A.J. Baca, K.J. Yu, J. Xiao, S. Wang, J. Yoon, J.H. Ryu, D. Stevenson, R.G. Nuzzo, A.A. Rockett, Y. Huang, J.A. Rogers, Energy Environ. Sci. 3 (2010) 208–211.
[73] J. Viventi, D.-H. Kim, L. Vigeland, E.S. Frechette, J.A. Blanco, Y.-S. Kim, A.E. Avrin, V.R. Tiruvadi, S.-W. Hwang, A.C. Vanleer, D.F. Wulsin, K. Davis, C.E. Gelber, L. Palmer, J. Van der Spiegel, J. Wu, J. Xiao, Y. Huang, D. Contreras, J.A. Rogers, B. Litt, Nat. Neurosci. 14 (2011) 1599–1605.
[74] D.-H. Kim, N. Lu, R. Ghaffari, Y.-S. Kim, S.P. Lee, L. Xu, J. Wu, R.-H. Kim, J. Song, Z. Liu, J. Viventi, B. de Graff, B. Elolampi, M. Mansour, M.J. Slepian, S. Hwang, J.D. Moss, S.-M. Won, Y. Huang, B. Litt, J.A. Rogers, Nat. Mater. 10 (2011) 316–323.
[75] D.-H. Kim, Y.-S. Kim, J. Wu, Z. Liu, J. Song, H.-S. Kim, Y.Y. Huang, K.-C. Hwang, J.A. Rogers, Adv. Mater. 21 (2009) 3703–3707.
[76] S.-W. Hwang, H. Tao, D.-H. Kim, H. Cheng, J.-K. Song, E. Rill, M.A. Brenckle, B. Panilaitis, S.M. Won, Y.-S. Kim, Y.M. Song, K.J. Yu, A. Ameen, R. Li, Y. Su, M. Yang, D.L. Kaplan, M. R. Zakin, M.J. Slepian, Y. Huang, F.G. Omenetto, J.A. Rogers, Science 337 (2012) 1640–1644.
[77] L. Sun, G. Qin, J.-H. Seo, G.K. Celler, W. Zhou, Z. Ma, Small 6 (2010) 2553–2557.
[78] S.W. Lee, K.S. Min, J. Jeong, J. Kim, S.J. Kim, IEEE Trans. Biomed. Eng. 58 (2011) 2255–2263.
[79] G. Gustafsson, Y. Cao, G.M. Treacy, F. Klavetter, N. Colaneri, A.J. Heeger, Nature 357 (1992) 477–479.
[80] T.-H. Han, Y. Lee, M.-R. Choi, S.-H. Woo, S.-H. Bae, B.H. Hong, J.-H. Ahn, T.-W. Lee, Nat. Photonics 6 (2012) 105–110.
[81] M.C. Choi, Y. Kim, C.S. Ha, Prog. Polym. Sci. 33 (2008) 581–630.
[82] F.A. Ponce, D.P. Bour, Nature 386 (1997) 351–359.
[83] D.A. Gaul, W.S. Rees Jr., Adv. Mater. 12 (2000) 935–946.
[84] J.Y. Tsao, M.E. Coltrin, M.H. Crawford, J.A. Simmons, Proc. IEEE 98 (2010) 1162–1179.
[85] E.F. Schubert, J.K. Kim, Science 308 (2005) 1274–1278.
[86] K.J. Jeon, S.-J. Kim, K.K. Park, J.-W. Kim, G. Yoon, J. Biomed. Opt. 7 (2002) 45–50.
[87] E.R.M. de Haas, H.C. de Vijlder, H.J.C.M. Sterenborg, H.A. M. Neumann, D.J. Robinson, J. Eur. Acad. Dermatol. Venereol. 22 (2008) 426–430.
[88] K.J. Lee, J. Lee, H. Hwang, Z.J. Reitmeier, R.F. Davis, J.A. Rogers, R.G. Nuzzo, Small 1 (2005) 1164–1168.
[89] M.A. Meitl, Z.-T. Zhu, V. Kumar, K.J. Lee, X. Feng, Y.Y. Huang, I. Adesida, R.G. Nuzzo, J.A. Rogers, Nat. Mater. 5 (2005) 33–38.
[90] K.J. Lee, M.a. Meitl, J.-H. Ahn, J.A. Rogers, R.G. Nuzzo, V. Kumar, I. Adesida, J. Appl. Phys. 100 (2006) 124507.
[91] I. Choi, H.Y. Jeong, D.Y. Jung, M. Byun, C. Choi, B.H. Hong, ACS Nano 8 (2014) 7671–7677.
[92] P.C. van der Wilt, M.G. Kane, A.B. Limanov, A.H. Firester, L. Goodman, J. Lee, J.R. Abelson, A.M. Chitu, J.S. Im, MRS Bull. 31 (2011) 461–465.
[93] M.G. Kane, A.H. Firester, L.A. Goodman, P.C. van der Wilt, A. B. Limanov, J.S. Im, in: Proceedings of SID Symposium Digest of Technical Papers, vol. 37, 2006, pp. 1365–1367.
[94] R. Delmdahl, R. Pätzel, J. Brune, Phys. Procedia 41 (2013) 241–248.
[95] S.H. Lee, S.Y. Park, K.J. Lee, Proc. SPIE 8460 (2012) 846011.
[96] S. Kim, J.H. Son, S.H. Lee, B.K. You, K.-I. Park, H.K. Lee, M. Byun, K.J. Lee, Adv. Mater. 26 (2014) 7480–7487 http://dx.doi.org/10.1002/adma.201402472.
[97] T. Kim, Y.H. Jung, J. Song, D. Kim, Y. Li, H. Kim, I.-S. Song, J.J. Wierer, H.A. Pao, Y. Huang, J.A. Rogers, Small 8 (2012) 1643–1649.
[98] J. Chun, Y. Hwang, Y.-S. Choi, J.-J. Kim, T. Jeong, J.H. Baek, H.C. Ko, S.-J. Park, Scr. Mater. 77 (2014) 13–16.
[99] D.-H. Kim, R. Ghaffari, N. Lu, J.A. Rogers, Annu. Rev. Biomed. Eng. 14 (2012) 113–128.
[100] M. Lee, C.Y. Chen, S. Wang, S.N. Cha, Y.J. Park, J.M. Kim, L.J. Chou, Z.L. Wang, Adv. Mater. 24 (2012) 1759–1764.
[101] J. Fang, H. Niu, H. Wang, X. Wang, T. Lin, Energy Environ. Sci. 6 (2013) 2196–2202.
[102] S. Pan, Z. Yang, P. Chen, J. Deng, H. Li, H. Peng, Angew. Chem. – Int. Ed. 53 (2014) 6110–6114.
[103] J. Zhong, Y. Zhang, Q. Zhong, Q. Hu, B. Hu, Z.L. Wang, J. Zhou, ACS Nano 8 (2014) 6273–6280.
[104] S.J. Kim, J.H. We, B.J. Cho, Energy Environ. Sci. 7 (2014) 1959–1965.

[105] S. Jung, J. Lee, T. Hyeon, M. Lee, D.-H. Kim, Adv. Mater. 26 (2014) 6329–6334.
[106] C.K. Jeong, K.M. Baek, S. Niu, T.W. Nam, Y.H. Hur, D.Y. Park, G.-T. Hwang, M. Byun, Z.L. Wang, Y.S. Jung, K.J. Lee, Nano Lett. 14 (2014) 7031–7038.
[107] G.-T. Hwang, M. Byun, C.K. Jeong, K.J. Lee, Adv. Healthcare Mater. (2014). http://dx.doi.org/10.1002/adhm.201400642.

Seung Hyun Lee received his B.S. degree in Materials Science and Engineering (MSE) from Sungkyunkwan University (SKKU) in 2011, M.S. degree from KAIST in 2013, and is a Ph.D. candidate in MSE at KAIST, under the supervision of Prof. Keon Jae Lee. His doctoral research interests include experimental and theoretical studies on inorganic-based flexible light-emitting diodes (LEDs), optoelectronics for biomedical applications, optogenetics, and laser lift-off (LLO) process.

Chang Kyu Jeong received his B.S. degree in Materials Science and Engineering (MSE) from Hanyang University in 2011 and M.S. degree from KAIST in 2013. He is currently a Ph.D. candidate in MSE at KAIST. He is working as a graduate researcher at Prof. Keon Jae Lee's group. His doctoral research topics focus on mechanical energy harvesting, soft/biomaterials, surface chemistry, and nanomaterial synthesis.

Geon-Tae Hwang is a Ph.D. candidate supervised in Materials Science and Engineering (MSE) at KAIST. He received his B.S. degree in MSE from Sungkyunkwan University (SKKU) in 2010 and M.S. degree from KAIST in 2012. His doctoral research focuses on flexible electronics (large scale integration, f-LSI) and flexible piezoelectric energy harvester for self-powered biomedical applications.

Prof. Keon Jae Lee received his Ph.D. in Materials Science and Engineering (MSE) at University of Illinois, Urbana-Champaign (UIUC). During his Ph.D. at UIUC, he involved in the first co-invention of "Flexible Single-Crystalline Inorganic Electronics", using top-down semiconductors and soft lithographic transfer. Since 2009, he has been a professor in MSE at KAIST. His current research topics are self-powered flexible electronic systems including energy harvesting/storage devices, LEDs, large scale integration (LSI), high density memory and laser material interaction for *in-vivo* biomedical and flexible applications.